Sustainable Advances in Construction and Building Materials

Sustainable Advances in Construction and Building Materials:

Achieving Net Zero

Edited by

B.B. Das, Salim Barbhuiya and Leon Black

Cambridge
Scholars
Publishing

Sustainable Advances in Construction and Building Materials:
Achieving Net Zero

Edited by B.B. Das, Salim Barbhuiya and Leon Black

This book first published 2025

Cambridge Scholars Publishing

Lady Stephenson Library, Newcastle upon Tyne, NE6 2PA, UK

British Library Cataloguing in Publication Data
A catalogue record for this book is available from the British Library

ISBN: 978-1-0364-4957-5
ISBN (Ebook): 978-1-0364-4958-2

CONTENTS

Self-Sensing Concrete - A New Generation Concrete for Structural Health Monitoring

Dr. C. Arvind Kumar[1],
Dr. Prathik Kulkarni[2]
and P. Ashveen Kumar[3]
[1, 3] Assistant Professor, Matrusri Engineering College, Hyderabad, Telangana
[2] Assistant Professor, Bajaj Institute of Technology, Wardha, Nagpur

Abstract

In this study, self-compacting concrete (SCC) is used to produce self-sensing concrete. Self-sensing concrete (SSC) is achieved by incorporating carbon fibres into SCC that utilises recycled coarse aggregate. The aim of this study is to reduce the consumption of natural aggregate and utilise waste-demolished aggregate by using recycled aggregate. Instead of conventional methods that involve embedding or attaching sensors at specific locations for structural health monitoring (SHM), SSC is developed as an alternative in this research. Concrete cubes utilising SSC are manufactured with varying dosages of multi-walled carbon nanotubes (MWCNT), ranging from 0% to 0.15% by weight of cement. The mechanical and stress-sensing properties of these specimens are investigated. The mechanical properties like compressive strength and split tensile strength tests, while the stress sensing test involves cyclic loading of the cubes for five cycles within the elastic range. The stress and fractional change in electrical resistance (FCR) data are plotted to assess the concrete's ability to sense stress under external loading.

The results indicate that increasing the dosage of carbon fibres improves the mechanical properties of the concrete. Regarding the stress sensing test,

concrete with a 0.1% dosage demonstrates a significant correlation between stress and fractional change in electrical resistance (FCR) compared to other dosages.

Keywords: Self-sensing concrete (SSC), Self-Compacting concrete (SCC), Multi-walled carbon nanotubes (MWCNT), Fractional change in resistance (FCR), Recycled coarse aggregate.

1. Introduction

The recent earthquake in Turkey-Syria has resulted in the tragic loss of over 40,000 lives. While earthquakes cannot be stopped or controlled, the implementation of structural health monitoring (SHM) techniques can help mitigate the loss of life and property. SHM enables the identification of weak structures, allowing for timely repairs or demolitions to prevent catastrophic failures during earthquakes and thereby reducing casualties. Therefore, SHM clearly needs to minimise such losses in the future. Various SHM techniques have been developed (Azimi & Pekcan, 2020; Di Nuzzo et al., 2021; Gómez et al., 2020; Mieloszyk et al., 2021), including embedding sensors within concrete or attaching them to the external surface where strain, stress, deflection, etc., need to be monitored. However, these traditional approaches to SHM only provide localised information based on the sensor locations and do not cover the entire structure. To enable comprehensive SHM of entire structures, a new technique called self-sensing concrete (SSC) is required. In SSC, the concrete itself is transformed into a sensor instead of relying on external or internal sensors. The concept of self-sensing concrete originated in the early 1990s when DDL Chung discovered that adding electrically conductive carbon fibres to cement resulted in a specimen capable of sensing external loads through measurements of its electrical resistance (Chen & Chung, 1993). This breakthrough laid the foundation for self-sensing concrete. Since then, numerous studies have explored the addition of carbon fibres (Cholker & Tantray, 2020), multi-walled carbon nanotubes (MWCNT) (Yoo et al., 2018), carbon black (Guo et al., 2022), combinations of carbon fibres and multi-walled carbon nanotubes (Park et al., 2018), and combinations of steel fibres and carbon fibres(Dehghani & Aslani, 2020).

Suchorzewski et al. (Suchorzewski et al., 2020) discovered that adding multi-walled carbon nanotubes (MWCNT) to high-performance concrete improves its mechanical properties and self-sensing capabilities. They found that even a small amount of MWCNT (0.05% and 0.10%) enhances

stress detection and allows for the monitoring of microcracking. In another study, Song et al. (S. Song et al., 2022) observed that carbon nanotube-reinforced concrete subjected to freeze-thaw cycles experienced a gradual decrease in peak stress and a slight increase in strain. The stress-strain curve shifted downward and to the right.

Gao et al. (Gao et al., 2020) studied the effect of adding 0.1% MWCNT and replacing natural aggregates with recycled concrete aggregates (RCA) on the strength of recycled aggregate concrete (RAC). Treated RAC samples showed a significant 42% increase in compressive strength compared to untreated samples. Song et al. (X. bin Song et al., 2021) investigated the impact of MWCNT on the interfacial mechanical properties of RAC. The addition of 0.2% MWCNT resulted in a 53% improvement in shear strength compared to mixtures without nano-tubes in a study by I. Murali et al. (Murali et al., 2021), the addition of 0.2% MWCNT in fibrous concrete led to a denser concrete matrix by filling nanopores.

The literature review reveals that previous studies on self-sensing concrete have primarily focused on cement, mortar specimens, and conventional concrete. Consequently, there is a need to investigate the behaviour of concrete with conductive fibres under real-world site conditions. Furthermore, in the current era, self-compacting concrete (SCC) has become widely used. Therefore, this study aims to explore the potential of self-sensing concrete to address sustainability concerns by manufacturing it using SCC and incorporating recycled coarse aggregate. A sufficient number of SCC specimens embedded with varying dosages of multi-walled carbon nanotubes (MWCNT) were cast and subjected to testing for both mechanical properties and stress-sensing capability under cyclic loading.

2. Experimental Work

2.1 Materials and Mixing

2.1.1 Materials Used

In the present study, Multi-Walled Carbon Nano-tubes (MWCNT) obtained from Sun Young Industry, South Korea, were used for the production of self-sensing concrete. These MWCNTs exhibit complete electrical conductivity, and their properties are listed in Table 1.

Table 1: Properties of MWCNT

Property	Purity	Colour	Length (mm)	Inner Diameter (nm)
Value	>94%	Black	Jun-16	05-Oct

Outer Diameter (nm)	True Density (g/cm^3)	Bulk Density (g/cm^3)	SSA (m^2/g)	Pore Volume (cm^3/g)
40-60	~2.2	~0.12	45-600	81

In this study, cement of grade 43 with a specific gravity of 3.14 was used to produce self-sensing concrete (SSC). The coarse aggregate employed in this research was obtained from nearby demolished structures. The concrete waste was screened and cleaned to obtain the selected aggregate, which had a size of 10mm and a specific gravity of 2.75 after the cleaning and sieving process. River sand, with a fineness modulus (FM) of 2.8 and a specific gravity of 2.65, was used as the fine aggregate. To ensure proper dispersion of the nano-tubes and achieve self-compacting concrete (SCC), a high-range water-reducing superplasticiser, which is PCE-based and has a density of 1.08 g/ml, was utilised. The mixing and curing of the concrete were carried out using tap water with a pH of 7.2."

2.1.2 Mix proportion

Self-compacting concrete (SCC) mixes were prepared by incorporating varying dosages of Multi-Walled Carbon Nano-tubes (MWCNT) ranging from 0% to 0.15% by weight of cement in 0.05% increments. The mix

proportions used for each dosage are presented in Table 2. Through multiple trials, an SCC mix with a target compressive strength of 40N/mm^2 was selected to ensure that both the hardened and fresh properties met the requirements of the EFNARC code (EFNARC, 2002). The material proportions for the self-compacting concrete without MWCNT, which served as the reference mix after conducting adequate trials, are also presented in Table 2, denoted as "Reference". Additionally, the table includes the flow properties of the different mixes after the addition of MWCNT. The flow properties were evaluated using the slump flow test specified by the EFNARC code, and it was observed that the slump flow of all the mixes remained within the prescribed limits.

Table 2: Material proportions and slump flow results

Specimen ID	Materials used in kg/m^3							Slump flow test in mm	
	MWCNT		Cement	Fine aggregate	Coarse aggregate	Water	Super Plasticizer (1.0%)	Experimental	Range as per EFNARC
	%	kg							
Reference	0	0	520	920	850	182	9.36	690	600-850
SCC-0.05	0.05	0.26	520	920	850	182	9.36	682	600-850
SCC-0.1	0.1	0.52	520	920	850	182	9.36	670	600-850
SCC-0.15	0.15	0.78	520	920	850	182	9.36	647	600-850

2.1.3 Specimen Preparation

To disperse the MWCNT, an initial solution was prepared by combining 50% of the water required for concrete preparation with Sodium Dodecylbenzene Sulfonate (SDBS) powder at a dosage of 0.15% by weight of the nano-tubes. The MWCNT were added to this solution, and the mixture was agitated using a mechanical churner for 15 minutes to ensure proper dispersion of the nanotubes in water. Subsequently, this dispersed

solution was added to the concrete mixer along with the dry cement, fine aggregate (FA), and coarse aggregate (CA). Simultaneously, a solution containing the remaining 50% of the water and the superplasticiser was also added. The concrete mixer was then used to mix the ingredients further until the desired self-compacting concrete consistency was achieved. After preparing the fresh mix, its fresh properties were evaluated using the slump flow test before transferring it to steel moulds of cubes and cylinders. The cubes had dimensions of 150 x 150 x 150 mm^3, while the cylinders had a diameter of 150 mm and a length of 300 mm. The fresh mix was poured into the moulds and left to dry at room temperature for 24 hours. Afterwards, the specimens were de-moulded and placed in fresh water for a curing period of 28 days. A total of five cubes and three cylinders were manufactured for each mix, ensuring an adequate sample size for testing and analysis.

2.2 Testing Procedure

2.2.1 Compressive and Split tensile strength

After the 28-day curing period, the specimens were taken out from the water and subjected to testing to determine their ultimate load-carrying capacity in both compression and tension. A Universal Testing Machine (UTM) was employed for this purpose. To evaluate the ultimate load-carrying capacity in compression, a set of three cubes was incrementally loaded using the UTM until failure occurred. Subsequently, the average stress value of the three specimens was calculated and recorded as part of the results. Similarly, to assess the split tensile strength of the SSC, the cylinders were loaded transversely using the UTM until failure, resulting in the specimens splitting into two pieces. The split tensile strength value was then calculated using the codal formula and included in the results section.

2.2.2 Electrical Resistivity Measurements

To ensure consistent measurement of electrical resistance across the specimens, an electrically conductive paint is applied along the periphery of the cubes. Copper wire is then wound over the paint, maintaining a 10mm distance from the top and bottom edges, as depicted in Figure 4. For electrical resistance measurements in both loaded and unloaded conditions, the top and bottom ends of the copper wires are connected to a digital multimeter (DMM). The initial electrical resistance is measured to assess the sensor's sensing capability prior to loading. To evaluate the strain-sensing ability, the resistance is measured during cyclic loading and unloading.

3. Results and Discussions

3.1 Mechanical Properties

3.1.1 Compressive strength

The ultimate load carrying capacity was tested to evaluate the influence of MWCNT on the strength of the concrete. For each MWCNT dosage, a set of three cubes was subjected to a gradual loading process using a Universal Testing Machine (UTM) with a 1000kN capacity. The loading was conducted at a constant speed of 5.2kN/sec until failure occurred. The maximum load-carrying capacity was recorded for each set, and the average values for each MWCNT dosage are presented in Table 3 for both compressive and split tensile strength.

Table 3: Compressive and split tensile strength results

Si. No	Specimen ID	Compressive Strength			Split Tensile Strength			Slump flow test in mm	
		Ultimate Load (kN)	Compressive Stress (N/mm^2)	% increase in stress	Ultimate Load (kN)	Compressive Stress (N/mm^2)	% increase in stress	Experimental	Range as per EFNARC
1	Reference	956.3	42.5	-	223.3	3.16		690	600-850
2	SCC-0.05	969.8	43.1	1.47	226.2	3.2	1.51	682	600-850
3	SCC-0.1	984.6	43.76	2.97	230.4	3.26	3.2	670	600-850
4	SCC-0.15	1001	44.48	4.67	234	3.31	4.9	647	600-850

Based on the results, it can be concluded that the addition of MWCNT positively impacts the compressive strength of the concrete. The increase in compressive strength is directly proportional to the dosage of MWCNT added to the mix, with the highest increase observed for the 0.15% dosage. The increase in compressive strength is 1.47% for a 0.05% dosage, 2.97% for a 0.1% dosage, and 4.67% for a 0.15% dosage compared to the compressive strength of the reference concrete. Figure 1 provides a

graphical representation of the compressive strength and the corresponding increase. This increase in strength can be attributed to the filling of pores within the concrete structure, resulting in a denser matrix due to the small size of the MWCNT. Additionally, these fibres contribute to bridging cracks in the concrete, further enhancing its strength. However, it is important to note that the observed increase in strength is relatively small.

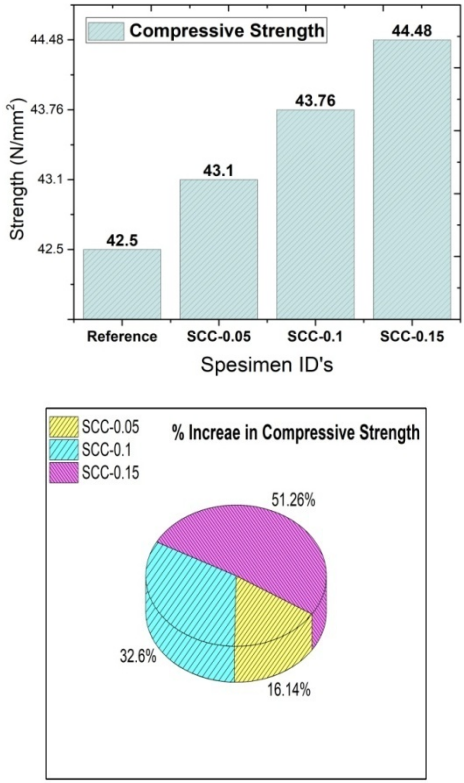

Figure 1: Increase in Compressive Strength

For split tensile strength, three cylinders were tested for each MWCNT dosage, and the averages are shown in Table 3. The results confirm that there is an increase in tensile strength with the addition of MWCNT. The split tensile strength of the cylinders with a dosage of 0.05% MWCNT increased by 1.51%. Similarly, for specimens with dosages of 0.1% and 0.15%, the increase in split tensile strength was 3.2% and 4.9%,

respectively. Figure 2 provides a graphical representation of the split tensile strength and the corresponding increase. Interestingly, the split tensile strength values are higher compared to the compressive strength values for the same MWCNT dosages. For example, while the increase in compressive strength from 0% to 0.1% dosage was 2.97%, the increase in split tensile strength for the same dosage of MWCNT was 3.2%. Similarly, at a dosage of 0.15%, the increase in compressive strength compared to the reference specimen was 4.67%, whereas the increase in split tensile strength was 4.9%.

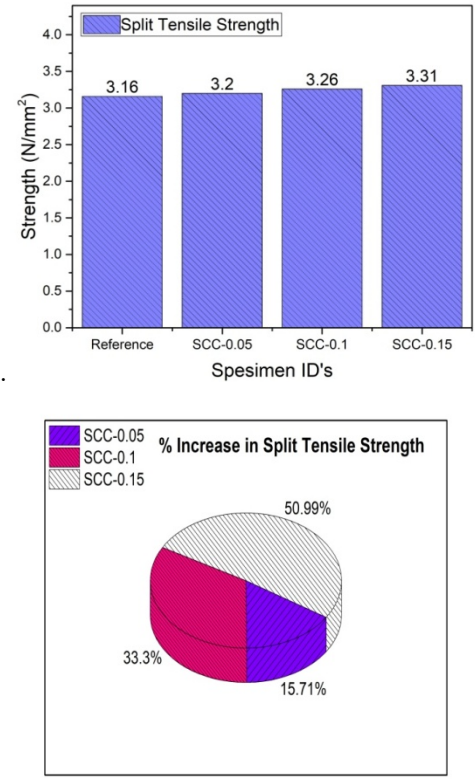

Figure 2: Split Tensile Strength

Based on these results, it can be concluded that the addition of MWCNT has a greater impact on the tensile strength of the concrete than the compressive strength when using the same dosage of MWCNT. This is attributed to the

behaviour of concrete under tensile loading, where cracks tend to form and the concrete tends to separate. The presence of MWCNT in the concrete acts as a bridging mechanism, effectively holding the concrete together and enhancing its tensile strength. As a result, the concrete exhibits improved resistance to cracking and increased overall strength in tension.

3.2 Electrical Properties

3.2.1 Initial Resistance

In order to evaluate the conversion of normal concrete to sensing concrete and its sensing ability, the initial resistance of all specimens with varying dosages of MWCNT was measured. To assess the conversion of normal concrete to sensing concrete and its sensing ability, the initial resistance of the specimens with different dosages of MWCNT was measured. The initial resistance was determined in a dry condition before subjecting the specimens to any loading. Figure 3 presents the measured values of initial resistance for various dosages of MWCNT across all the specimens. The plot clearly demonstrates that as the dosage of MWCNT increases, the electrical resistance decreases, indicating an enhanced sensing capability of the concrete compared to the reference sample. For the reference concrete, the initial resistance was measured at 332 k-ohms, while for the specimens containing 0.05% MWCNT, the resistance drastically reduced to 48 k-ohms. Beyond the 0.05% dosage, the change in resistance was relatively small. These results indicate that the addition of MWCNT to the reference concrete successfully transformed it into a sensor, exhibiting improved electrical conductivity and sensing properties.

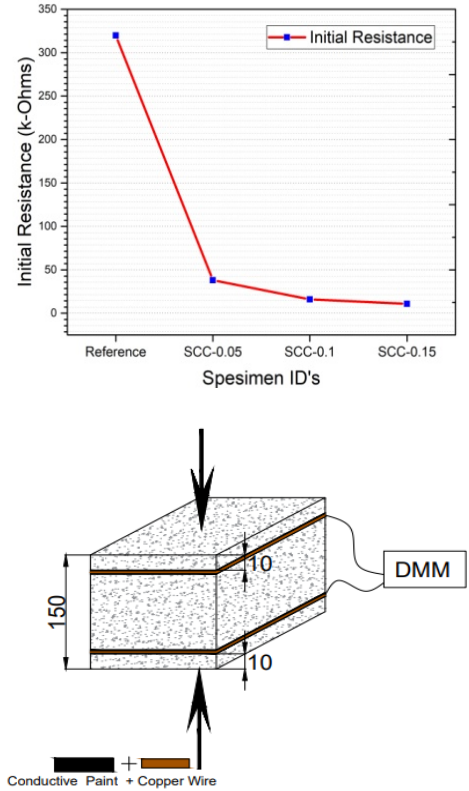

Figure 3: Initial Electrical Resistance; 4. Specimen and Setup

3.2.2 Stress sensing test

To check the stress sensing ability of the specimen, as mentioned previously, it was loaded in a cyclic manner for 5 cycles, with a peak load of 382kN. This load was set based on 40% of the peak load-carrying capacity of the reference sample, and the cyclic load remained within the elastic limit. During testing, the load and electrical resistance were measured, and a plot of stress and fractional change in resistance (FCR) was generated, as shown in Fig. 5. The stress was calculated using the load, while the FCR was determined using the equation shown below as equation 1.

$$FCR = \frac{\Delta R}{R} = \frac{R_x - R_0}{R_0} \quad (1)$$

In the equation mentioned above, Rx represents the electrical resistance of the sample at any given time during the loading process, while R_0 represents the initial resistance of the sample.

Figure 5 depicts a plot with time on the x-axis and FCR (fractional change in resistance) and stress on the y-axis. During the cyclic loading, both the stress and FCR values were calculated and plotted accordingly. The results obtained from Figure 5 reveal important observations. For the reference sample, as shown in Figure 5(a), there is no significant variation in the FCR readings during cyclic loading. This indicates that the reference sample, without the addition of MWCNT, did not exhibit any sensing ability to external loading. The FCR readings remained relatively constant, and there was no correlation between FCR and stress. This confirms that the absence of MWCNT prevented the specimen from being converted into a sensor. In contrast, the specimen with 0.05% MWCNT, as illustrated in Figure 5(b), shows an observable improvement in the FCR plot compared to the reference sample. The FCR plot demonstrates variation during both increasing and decreasing loading, indicating the sensing ability induced by the addition of MWCNT. Although the variation in FCR is not as precise as the cyclic stress, it does show discernible changes. Additionally, the correlation between stress and FCR improves with a higher dosage of MWCNT. The FCR tends to increase with increasing loading and decrease with decreasing loading. This behaviour can be attributed to the movement of the dispersed MWCNT in the concrete specimen during loading, leading to a decrease in electrical resistance and an increase in conductivity. In summary, Figure 5 provides evidence that the addition of MWCNT to the concrete specimen enhances its sensing ability to external loading. The FCR readings exhibit variation and demonstrate a correlation with the applied stress, indicating the conversion of the specimen into a sensor.

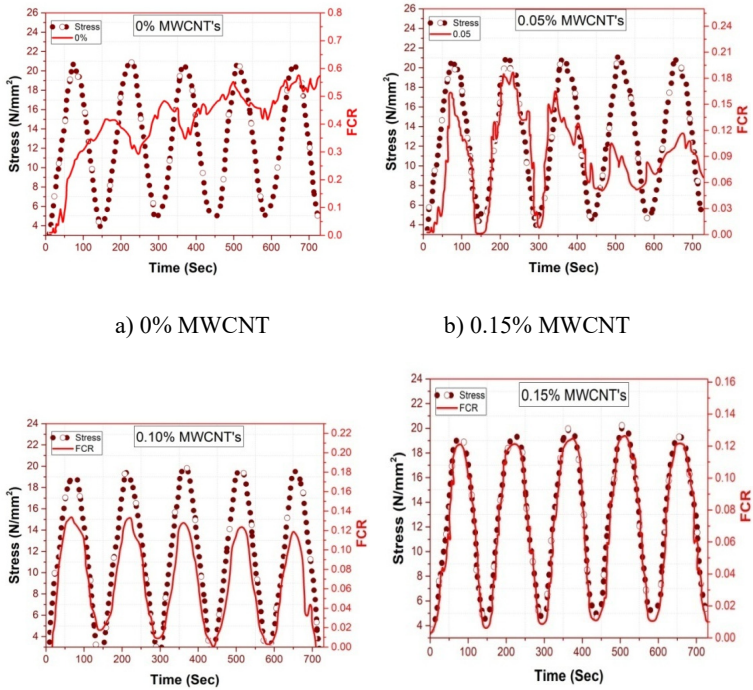

a) 0% MWCNT b) 0.15% MWCNT

c) 0.10% MWCNT d) 0.15% MWCNT

Figure 5: Plot of Stress and FCR against time

Similarly, during the unloading phase, the dispersed MWCNT fibres move away from each other due to the decrease in applied load. This movement results in a reduction in the flow of ions and an increase in electrical resistance. For the specimen with a dosage of 0.1% MWCNT, the FCR plot shown in Figure 5(c) demonstrates further improvement in stress sensing compared to the reference and 0.05% MWCNT specimens. The increased sensing ability is attributed to the enhanced dispersion of MWCNT within the concrete specimen. Additionally, the FCR plot exhibits a pattern of variation similar to that of the stress plot and aligns closely with it. Regarding the specimen with a dosage of 0.15% MWCNT, the stress sensing ability also improves, but the difference compared to the 0.1% MWCNT specimen is not significantly pronounced, as depicted in Figure 5(c). Considering economic considerations, a dosage of 0.1% MWCNT can be considered sufficient for producing self-sensing concrete, as it provides

substantial improvements in stress sensing without the need for higher MWCNT dosages.

Self-sensing concrete holds significant potential to revolutionise structural monitoring for stress and damage. Its real-time stress measurement capabilities, without the need for structural dismantling, can greatly enhance infrastructure safety and maintenance. Continuous Structural Health Monitoring (SHM) can be achieved throughout the entire structure without the requirement of attaching or inserting sensors at specific locations. This advancement has the capacity to improve overall structural safety and durability by enabling timely detection and mitigation of stress and damage.

4. Conclusions

1. The incorporation of recycled coarse aggregate in the production of self-sensing concrete offers the potential to reduce the demand for natural coarse aggregate. Furthermore, the addition of MWCNT does not significantly impact the fresh properties of self-compacting concrete.
2. The introduction of MWCNT into the concrete results in improved strength, as demonstrated by the increase in both compressive and split tensile strength. The compressive strength shows enhancements of 1.47%, 2.97%, and 4.67% for 0.05%, 0.1%, and 0.15% dosages of MWCNT, respectively. Likewise, the split tensile strength exhibits improvements of 1.51%, 3.2%, and 4.9% for the corresponding dosages of MWCNT.
3. The strain-sensing capability of the concrete increases with higher dosages of MWCNT during cyclic loading. The plot of stress and Fractional Change in Resistance (FCR) demonstrates the closest similarity at a dosage of 0.15%. However, considering economic factors, a dosage of 0.1% can be considered optimal as it does not exhibit a significant difference.
4. Consequently, this innovative self-sensing concrete incorporating recycled aggregate presents a more effective means of stress sensing compared to conventional structural health monitoring (SHM) techniques.

References

1. Azimi, M., & Pekcan, G. (2020). Structural health monitoring using extremely compressed data through deep learning. *Computer-Aided Civil and Infrastructure Engineering*, *35*(6).

https://doi.org/10.1111/mice.12517
2. Chen, P. W., & Chung, D. D. L. (1993). Carbon fibre reinforced concrete for smart structures capable of non-destructive flaw detection. *Smart Materials and Structures*, *2*(1). https://doi.org/10.1088/0964-1726/2/1/004
3. Cholker, A. K., & Tantray, M. A. (2020). Strain-sensing characteristics of self-consolidating concrete with micro-carbon fibre. *Australian Journal of Civil Engineering*, *18*(1). https://doi.org/10.1080/14488353.2019.1704206
4. Dehghani, A., & Aslani, F. (2020). The effect of shape memory alloy, steel, and carbon fibres on fresh, mechanical, and electrical properties of self-compacting cementitious composites. *Cement and Concrete Composites*, *112*, 103659. https://doi.org/10.1016/J.CEMCONCOMP.2020.103659
5. Di Nuzzo, F., Brunelli, D., Polonelli, T., & Benini, L. (2021). Structural Health Monitoring System with Narrowband IoT and MEMS Sensors. *IEEE Sensors Journal*, *21*(14). https://doi.org/10.1109/JSEN.2021.3075093
6. EFNARC. (2002). Specification and Guidelines for Self-Compacting Concrete. *Report from EFNARC*, *44*(February).
7. Gao, C., Huang, L., Yan, L., Jin, R., & Chen, H. (2020). Mechanical properties of recycled aggregate concrete modified by nano-particles. *Construction and Building Materials*, *241*, 118030. https://doi.org/10.1016/J.CONBUILDMAT.2020.118030
8. Gómez, J., Casas, J. R., & Villalba, S. (2020). Structural Health Monitoring with Distributed Optical Fibre Sensors of tunnel lining affected by nearby construction activity. *Automation in Construction*, *117*, 103261. https://doi.org/10.1016/J.AUTCON.2020.103261
9. Guo, Y., Li, W., Dong, W., Luo, Z., Qu, F., Yang, F., & Wang, K. (2022). Self-sensing performance of cement-based sensor with carbon black and polypropylene fibre subjected to different loading conditions. *Journal of Building Engineering*, *59*. https://doi.org/10.1016/j.jobe.2022.105003
10. Mieloszyk, M., Majewska, K., & Ostachowicz, W. (2021). Application of embedded fibre Bragg grating sensors for structural health monitoring of complex composite structures for marine applications. *Marine Structures*, *76*, 102903. https://doi.org/10.1016/J.MARSTRUC.2020.102903
11. Murali, G., Abid, S. R., Karthikeyan, K., Haridharan, M. K., Amran, M., & Siva, A. (2021). Low-velocity impact response of novel prepacked expanded clay aggregate fibrous concrete produced with

carbon nanotube, glass fibre mesh and steel fibre. *Construction and Building Materials*, *284*, 122749. https://doi.org/10.1016/J.CONBUILDMAT.2021.122749

12. Park, H. M., Kim, G. M., Lee, S. Y., Jeon, H., Kim, S. Y., Kim, M., Kim, J. W., Jung, Y. C., & Yang, B. J. (2018). Electrical resistivity reduction with pitch-based carbon fibre into multi-walled carbon nanotube (MWCNT)-embedded cement composites. *Construction and Building Materials*, *165*, 484–493. https://doi.org/10.1016/J.CONBUILDMAT.2017.12.205
13. Song, X. bin, Li, C. zhi, Chen, D. dan, & Gu, X. lin. (2021). Interfacial mechanical properties of recycled aggregate concrete reinforced by nano-materials. *Construction and Building Materials*, *270*, 121446. https://doi.org/10.1016/J.CONBUILDMAT.2020.121446
14. Song, S., Niu, Y., & Zhong, X. (2022). Study on dynamic mechanical properties of carbon nanotubes reinforced concrete subjected to freeze–thaw cycles. *Structural Concrete*, *23*(5). https://doi.org/10.1002/suco.202100464
15. Suchorzewski, J., Prieto, M., & Mueller, U. (2020). An experimental study of self-sensing concrete enhanced with multi-wall carbon nanotubes in wedge splitting test and DIC. *Construction and Building Materials*, *262*, 120871. https://doi.org/10.1016/J.CONBUILDMAT.2020.120871
16. Yoo, D. Y., You, I., & Lee, S. J. (2018). Electrical and piezoresistive sensing capacities of cement paste with multi-walled carbon nanotubes. *Archives of Civil and Mechanical Engineering*, *18*(2). https://doi.org/10.1016/j.acme.2017.09.007

EFFECTS OF CERAMIC POLISHING WASTE ON FLY ASH GEOPOLYMER CONCRETE

JAY BHAVSAR[1] AND VIJAY R. PANCHAL[1]
[1]M. S. PATEL DEPARTMENT OF CIVIL ENGINEERING,
CHANDUBHAI S. PATEL INSTITUTE OF TECHNOLOGY (CSPIT),
FACULTY OF TECHNOLOGY AND ENGINEERING, CHAROTAR
UNIVERSITY OF SCIENCE AND TECHNOLOGY (CHARUSAT)

Abstract

Geopolymer concrete (GPC) is an alternative to ordinary concrete due to its greater strength and endurance. In recent decades, fly ash-based GPC has attracted the interest of researchers. Additionally, the GPC provides alternatives for recycling industrial waste into concrete. Ceramic polishing waste (CPW) has alumino-silicate characteristics, which make it suitable as a geopolymer binder. This study substituted fly ash with CPW for the production of GPC. In the first stage, GPC is made with fly ash and CPW and cured for 24 hours at 60 °C. In the second stage, GPC was modified with the addition of ground-granulated blast furnace slag (GGBS) as a precursor, along with fly ash and CPW. The modified GPC blends are cured at room temperature. The essential properties of GPC, such as workability, density, compressive strength, acid resistance, and water absorption, were analysed using conventional test procedures. The carbon emissions of GPC were also investigated. The results showed the use of CPW in place of fly ash performed better at ambient temperature than in oven curing. The use of GGBS improved the strength at ambient temperature and also reduced the carbon emissions of GPC.

Keywords: Geopolymer, Temperature curing, Ambient curing, Ceramic Polishing Waste

1. Introduction

Concrete is one of the most in-demand building materials worldwide, and its demand in the construction industry will increase in the future. Concrete is typically made with Portland cement, which is widely used across the globe. Nonetheless, the infrastructure sector is showing interest in geopolymer concrete (GPC) studies because of their lower carbon footprint. In addition to being a superior replacement for industrial waste, GPC also offers other useful benefits. The most effective precursors for making geopolymer concrete are industry by-products, such as fly ash and ground-granulated blast furnace slag (GGBS). Past research has shown the use of other industrial wastes, such as rice husk ash, bagasse ash, ceramic polishing waste (CPW), and ceramic waste powder (CWP). In the last decade, significant research work has been carried out on ceramic wastes as geopolymer precursors due to their alumino-silicate properties. The use of ceramic waste in conventional concrete as a recycling material has shown fruitful results in terms of strength and durability.

The increased demand for ceramic products may increase the amount of waste materials generated, which requires attention to avoid land pollution, water pollution, and air pollution. One cubic meter of polished tiles resulted in approximately 1.9 kg of ceramic trash (El-Dieb et al., 2018). Many researchers used crushed ceramic tile powder in GPC (Huseien et al., 2020; Shoaei et al., 2019). The replacement of GGBS with crushed ceramic tile powder reduced the strength of GPC (Huseien et al., 2020). The geopolymer mortar developed with crushed ceramic tile powder at 105 ℃ had maximum strength (Shoaei et al., 2019). Aly et al., 2018 explored the possibilities of using ceramic waste as a potential geopolymer precursor. Geopolymer bricks were developed from ceramic dust. The authors reported high compressive strength (CS) of geopolymer bricks with longer curing duration, but it reduced at high curing temperatures (Amin et al., 2017). Ameri et al., 2019 discovered that a ceramic waste-based lightweight geopolymer mortar performed optimally at elevated temperatures. Red ceramic waste can be used with metakaolin to develop geopolymer paste (Sarkar and Dana, 2020). Azevedo et al., 2020 used red ceramic waste with metakaolin to make geopolymer roof tiles. The authors found that room curing takes more time in the strength gain process compared to temperature curing (Azevedo et al., 2020).

In earlier investigations, it was demonstrated that GGBS could be used with crushed ceramic tile powder to make geopolymer mortar, paste, or concrete. Also, different ceramic wastes were used as geopolymers to produce bricks

or tiles. The GPCs utilized CPW with fly ash have not been discussed concerning the alkaline liquid-to-binder (A/B) ratio. Also, CPW requires a lower energy input during the crushing process than crushed ceramic tile powder. In addition, only a few studies reported using CPW in GPC at room temperature with other precursors, such as fly ash and GGBS. Furthermore, past studies on CPW have not examined the impacts of oven curing, ambient curing, alkaline liquid, and superplasticizer (SP) on carbon emissions (CE), which are key factors for CE of GPC.

The study was carried out in two stages. Initially, oven curing was adopted to make GPC. The GPC mixes were prepared with a different A/B ratio, where fly ash was replaced by CPW. In the second stage, ambient curing was adopted, but the earlier mixes were modified by adding GGBS. The study shows that 15% of CPW can be used as a replacement for fly ash. The GGBS improved the performance of GPC at ambient temperatures. The high SP and high A/B ratio improved workability, but the high amount of alkaline liquid increased carbon emissions.

2. Materials

Fly ash, ceramic polishing waste (CPW), and GGBS were used as precursors in the study. The properties of precursors are presented in Table 1 and Table 2.

Table 1: Chemical properties of precursors

Materials	SiO_2	Al_2O_3	Fe_2O_3	CaO	MgO	Na_2O	K_2O	SO_3	P_2O_5	TiO_2
Fly ash	58.98	15.19	12.50	01.82	0.62	0.25	1.88	1.60	0.58	3.98
CPW	70.71	11.56	02.86	03.45	1.21	1.39	3.39	0.46	0.17	1.48
GGBS	35.41	17.60	01.62	37.58	7.60	-	-	0.75	-	-

Table 2: Physical properties of precursors

Precursor	Fly ash	CPW	GGBS
Specific Surface Area (cm^2/g)	5538	4976	448.1
Specific Gravity	2.500	2.529	2.880

For making GPC, coarse aggregates (CA) 10-20 mm in size were mixed with fine aggregates (FA). The fineness modulus of FA was 2.56. FA and CA have specific gravity values of 2.60 and 2.69, respectively. Both aggregates satisfied the requirements of the Indian standard (IS 383, 2016). Technical-grade sodium hydroxide (NaOH) flakes and sodium silicate (Na_2SiO_3) in liquid form were obtained for the study. NaOH solution of 14M was prepared for making GPC. Na_2SiO_3 with a SiO_2 to Na_2O proportion of 1.97 by mass was used. The SiO_2, Na_2O, and water percentages in the Na_2SiO_3 were 31.4%, 15.9%, and 52.7%, respectively.

3. Methodology

The literature survey was carried out to find the research gap. Figure 1 shows the methodology adopted for the research work. Seven mixes were prepared, including the control mix GC-1. GC-1 was made of 100% fly ash as a precursor and it was cured at 60 ℃ in the oven for 24 hours (h) (Table 3). The samples of GPC mix Nos. 1 to 5 were stored at room temperature for 24 h after casting. After that, the samples were cured at 60 ℃ in an oven for one day. The samples were cured at room temperature until testing. Mix No. 3 to 5 were modified by changing the A/B ratio from 0.35 to 0.45.

Mixes 6 and 7 were modified with the addition of 20% GGBS of total binder content and also cured at room temperature until testing (Table 3). In all the mixes, fly ash was partially replaced by CPW in different proportions (Table 3). The proportion of aggregates was constant for all mixes 1-7, which was 1848 kg/m^3. Out of total aggregates, FA was 45% and CA was 55%.

The workability, density, and compressive strength of GPC were investigated in the study. Also, the durability of GPC was measured through a water absorption and acid resistance test. The standard test procedures used for experimental work are listed in Table 4. For each test, three specimens were tested and average results were reported. The carbon emissions were also measured for designed mixes.

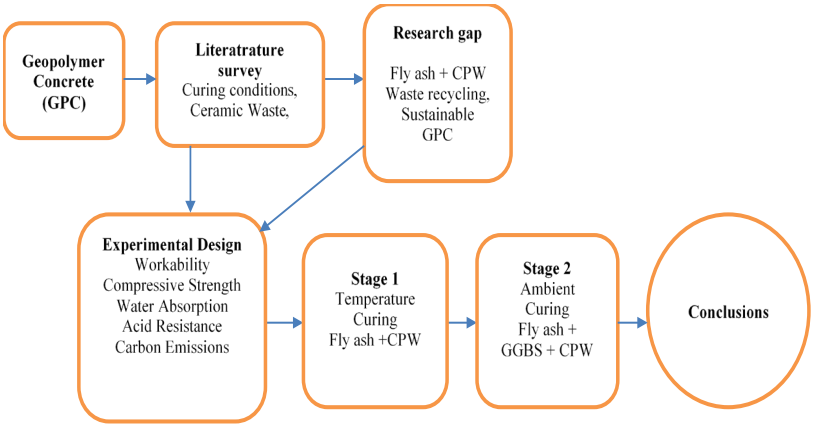

Figure 1: Research methodology

Table 3: Geopolymer concrete mix proportion (kg/m^3)

Mix No.	Mix	Fly Ash	CPW	GGBS	Na_2SiO_3	NaOH	A/B	SP	Curing
1.	GC-1	408.8	-	-	102.2	40.9	0.35	-	60 ℃
2.	GV15-1	347.5	61.3	-	102.2	40.9	0.35	-	60 ℃
3.	GV15-2	323.5	57.1	-	122.4	49.0	0.45	6.1	60 ℃
4.	GV30-2	245.5	114.2	-	122.4	49.0	0.45	6.1	60 ℃
5.	GV50-2	190.3	190.3	-	122.4	49.0	0.45	6.1	60 ℃
6.	SGV15-1	278.0	49.0	81.8	102.2	40.9	0.35	-	Ambient
7.	SGV20-1	261.6	65.4	81.8	102.2	40.9	0.35	6.1	Ambient

GC: Fly ash GPC, SG: Fly ash slag GPC, VXX: % of CPW, -1: 0.35 A/B ratio, -2: 0.45 A/B ratio

Table 4: Test procedure

Sr. No.	Name of Test	Standards	Testing time	Specimen Size	Specimen Shape
1.	Slump test	(IS 1199, 2018)	Fresh	-	-
2.	Compressive strength	(IS 516 Part 1/Sec 1, 2021)	7 and 28 days	150 mm	cube
3.	Water absorption	(ASTM C642-13, 2013)	56 days	100 mm diameter 50 mm height	cylinder
4.	Acid resistance	-	28 days acid immersion	150 mm	cube

4. Results analysis

4.1. Workability and Density

The workability of GPC was measured through a slump test. The subsidence of concrete was measured as a slump. The slump of GPC decreased with the increase of CPW. However, it increased with the increase of the A/B ratio from 0.35 to 0.45, and the use of a superplasticizer improved workability. The highest workability was obtained for the GV15-2 mix, and the lowest was obtained for SGV20-1 (Figure 1). This shows that the higher A/B ratio and superplasticizer improve the workability of GPC. Increasing CPW by more than 20% required an additional superplasticizer as the fresh mix became harsh. Past studies reported similar behaviour when the A/B ratio of geopolymer mortar was increased (Shoaei et al., 2019). Also, past studies reported an increase in GGBS in place of fly ash, which reduced workability (Nath and Sarker, 2014).